Egypt. J. Chem. **Vol.** 68, SI: Z. M. Nofal, pp. 995- 1007(2025)

Egyptian Journal of Chemistry

http://ejchem.journals.ekb.eg/

Synthesis and Application of Triketone-Based Vitrimers and Nanocomposites for Engineering Thermoplastic Blends

Khloud M. K. Omar[*1], Marwa S. S. Mohamed[2], Wael S. I. Abou-Elmagd [3], and Amna Ramzy[4]

[1]*Chemical Administration Centre, Cairo, Egypt*

[2]*Department of Pharmaceutical Chemistry, Faculty of Pharmacy and Biotechnology, German University in Cairo, Egypt*

[3]*Chemistry Department, Faculty of Sciences, Ain Shams University, Egypt*

[4]*Department of Materials Engineering, Faculty of Engineering and Materials Science, German University in Cairo, Egypt*

Abstract

Vitrimers combine the processability of thermoplastics with the strength and durability of thermosets through dynamic covalent bonds, enabling reshaping, repair, and recycling—key features for sustainable material systems. This study presents the synthesis of novel vitrimers based on triketone (TK) structures for advanced engineering applications. TK-based monomers were employed to prepare polydiketone (PDK) vitrimers and their corresponding nanocomposites. Structural variants derived from Azelaic acid (TK-AZ), Glutaric acid (TK-G), and Adipic acid (TK-AD) were synthesized and compared, along with their PDK counterparts. Among these, PDK-TK-G and its CNT nanocomposite demonstrated the highest glass transition temperatures (T_g), reaching 134.8 °C and 120.6 °C, respectively. These vitrimers exhibit excellent thermal processability and compatibility with thermoplastics. When incorporated into polyvinyl chloride (PVC) blends, PDK-TK-G increased the T_g of PVC from 86.37 °C to 141.45 °C, significantly enhancing its thermal stability. The resulting vitrimers, composites, and polymer blends were thoroughly characterized for thermal and chemical performance. This novel method enhances the thermal stability of PVC and substantially increases its suitability for diverse engineering applications, especially those demanding high heat resistance. This work contributes directly Industry and Innovation by fostering next-generation material technologies, and resource-efficient manufacturing.

Keywords: Vitrimer; Thermosets; Thermoplastics; Triketone; Polydiketone; PVC.

1. Introduction

Conventional plastics, classified into thermosets and thermoplastics, are widely used in everyday life. Thermosets, known for their resistance, are difficult to recycle, leading to significant plastic waste [1]. Thermoplastics, consisting of linear polymer chains without crosslinks, can be reshaped by heating multiple times without losing physical properties, but their mechanical performance decreases upon recycling [2]. Thermosets, used in various applications like automotive bodies, have structural stability due to irreversible chemical bonds but cannot be reprocessed or recycled [3, 4, 5]. Current waste management for thermosets involves landfilling, grinding, and combustion [6, 7].

Vitrimers, the new third class of plastics, combine dynamic covalent networks from thermosets and have the ability to change topology through bond exchange under external effects, making them suitable for thermal processing, reshaping, repairing, and recycling [8, 9, 10]. Covalent adaptable network (CAN) polymers exhibit both the excellent mechanical properties of thermosets and the reprocessability of thermoplastics, undergoing bond cleavage and reformation under external stimuli [11]. CANs can be classified based on dynamic reaction mechanisms, with common mechanisms being reversible addition rearrangements (dissociative exchange) and reversible exchange rearrangements (associative exchange), as shown in Fig. 1[12, 13]. Dissociative exchange involves breaking a covalent bond before forming a new one, while associative exchange forms a new bond first before breaking the original [10]. Dissociative exchange is advantageous as it lowers polymer viscosity, aiding recycling. It rearranges network strands, reducing connectivity and crosslinking density. Associative exchange retains connectivity and density, with equilibrium unaffected by temperature but reaction speed influenced. In contrast, dissociative exchange equilibrium depends on temperature, impacting bond breakage rates, crosslinking density, and formation [14].

Vitrimers are a new class of materials composed of covalently linked chains forming an organic network. This network can change its topology through thermally induced associative exchange reactions, providing thermal malleability. Vitrimers are classified based on the polymer networks used or their chemistry, fig. 2.

Polyketone (PK) is a new class of semicrystalline thermoplastic polymers synthesized by catalytic copolymerization of α-olefins with carbon monoxide in an alternating sequence [15, 16]. PK polymers exhibit excellent mechanical properties, including high tensile yield stress, impact performance, superior barrier properties, and high chemical resistance, making them

*Corresponding author e-mail: khloud_science@yahoo.com.; (Khloud Mohamed).

Received date 16 April 2025; Revised date 11 May 2025; Accepted date 11 June 2025

DOI: 10.21608/ejchem.2025.375299.11605

attractive for industrial applications. PDK vitrimers, based on dynamic covalent chemistry, are innovative plastics that maintain their properties through repeated use and recycling. They enable closed-loop recycling with low-cost, low-energy processes, minimizing environmental impact. Synthesized via polycondensation of ß-triketones and amines, PDKs form a dynamic network that is solid at room temperature but flows under heat and pressure, fig. 3 [17].

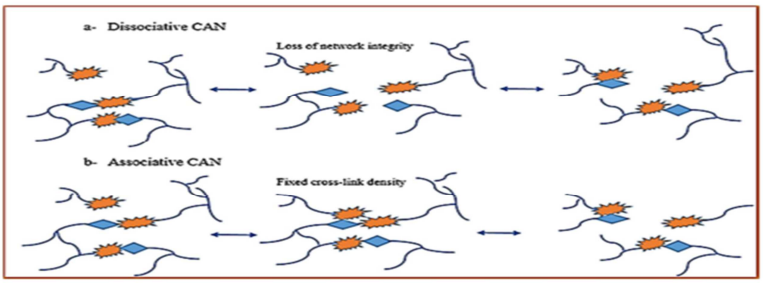

Figure 1: a) Dissociative exchange and b) Associative exchange in dynamic covalent adaptive networks. [10]

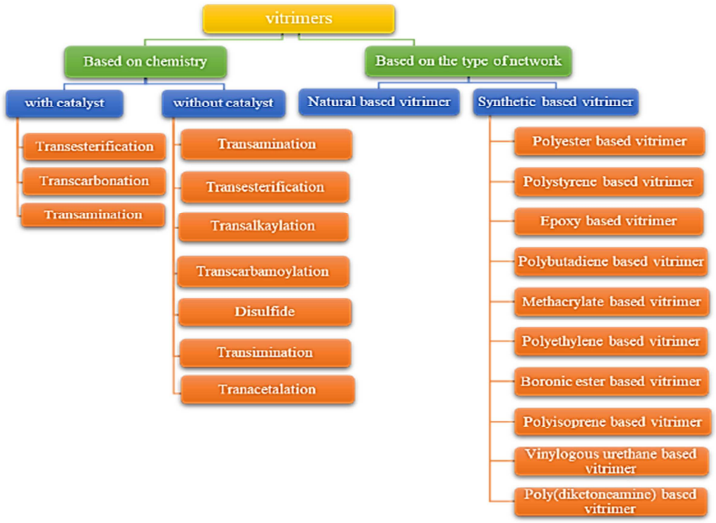

Figure 2: Vitrimer classification

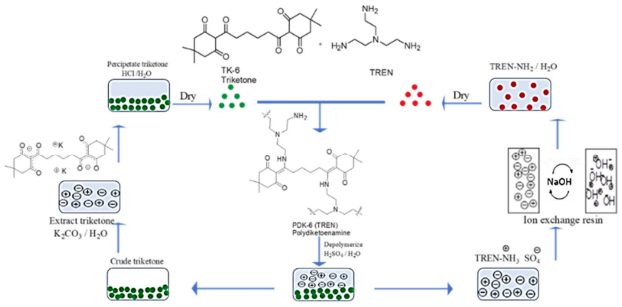

Figure 3: Closed-loop recycling from dynamic covalent PDKs [17].

Vitrimer/CNT composites:

Efforts to develop sustainable, high-performance materials have led to the creation of carbon material/vitrimer composites, combining carbon fillers like graphene, carbon fibers, and CNTs to enhance properties like strength, conductivity, and recyclability. [18-20], vitrimers reorganize their crosslinks at high temperatures, maintaining density. Carbon fillers, particularly graphene, carbon fibers, and CNTs, dominate this field.

Carbon nanotubes (CNTs) enhance polymer composites' mechanical and electrical properties, offering stimuli-responsiveness and other functionalities. They are incorporated into vitrimer composites via dispersion and curing, though aggregation issues require dispersal aids. Various modifications, like functional groups or coatings, improve CNT dispersion, interfacial bonding, and performance in composites. [21-30].

Vitrimer application:

Vitrimers, known for recyclability and dynamic properties, are used in robotics, aerospace, and automotive industries. They provide functionalities such as recycling, self-healing, and shape memory via dynamic covalent bonds. They also enhance 3D printing by enabling recyclable and robust materials [10, 14, 31-43].

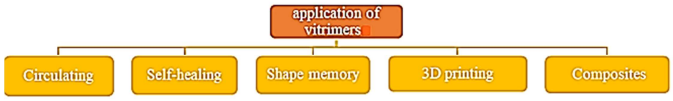

Figure 4: Vitrimer applications

2. Experimental:

2.1. MATERIALS:

5,5-dimethyl-1,3-cyclohexanedione (**dimedone**) 95% (Case no. 126-81-8), N,N'-dicyclohexylcarbodiimide (**DCC**) 99% (Cas no. 538-75-0), 4-dimethylaminopyridine (**DMAP**) ≥ 99% (Case no. 1122-58-3), tris(2-aminoethyl)amine (**TREN**) 96% (Case no. 4097-89-6), Adipic acid 99% (Case no. 124-04-9), and Dichloromethane (**DCM**) 99.9% (Case no. 75-09-2), Cyclohexanone 99% (Case no. 108-94-1), Ethanol 99% (Case no. 64-17-5) were purchased from Sigma-Aldrich. Azelaic acid 97.5% (Case no. 123-99-9), and Glutaric acid 99% (Case no. 110-94-1) were purchased from Loba Chemie PVT.LTD. Ethyl acetate 99.8% (Case no. 141-78-6), and n-hexane 90% (Case no. 110-54-3) were kindly supplied by Brouge Company. Hydrochloric acid (HCl fuming) 37% (Case no. 7647-01-0) was purchased from EMSURE EMD Millipore Corporation. Magnesium Sulphate (Heptahydrate) 99% (Case no. 10034-99-8) was purchased from Oxford LAB FINE CHEM LLP, MWCNT NC7000TM (CNT loading 100%) from nanocyl, PVC from ONGROW Cooperation.

2.2. INSTRUMENTATION:

- FT-IR spectra were collected using Nicolet IS50 FT-IR, IS50 ATR, Wavenumber range (500-4000 cm-1), number of scan per sample: 16, Resolution: 2, was performed by Chemistry Adminstration.
- EI Mass Spectra were recorded on UPLC-ESI-MS using waters ACQUITY xevo TQD system, was performed by Faculty of Pharmacy, GUC.
- Solution-Phase Nuclear Magnetic Resonance (NMR) ^{1}H NMR spectra were recorded on Burker alpha 2 NMR Advance HD III at 1500Mz and 100 MHz, respectively. Chemical shifts are reported in δ (ppm) relative to the residual solvent peak ($CDCl_3$: 7.26 for 1 H). Splitting patterns are designated as s (singlet), br s (broad singlet), d (doublet), t (triplet), q (quartet), and m (multiplet), was performed by Center of discovery research and development, Center of discovery research and development, Faculty of Pharmacy, Ain-Shams University.
- Density was estimated by ASTM D 792 method, Chemistry Administration.
- The thermal stability of the samples were investigated via the Perkin Elmer, Thermogravimetric analyzer TGA7 technique, USA. Samples were heated under Nitrogen at a rate of 10 °C/min from 25 to 600 ºC, HBRC.
- Differential scanning calorimetry, DSC Q2000 from TA Instruments, Temperature Range: -70 to 725°C, Temperature Accuracy: ± 0.1°C, Temperature Precision: ± 0.01°C, Calorimetric Precision (Indium Metal): ± 0.05%, High Sensitivity: (0.2 µW), Faculty of Engineering, Ain-Shams University.
- PerkinElmer DSC 4000, Temperature Range: -65 to 450°C, Temperature Accuracy: ± 0.1°C, Temperature Precision: ± 0.02°C, Calorimetric Precision (Indium Metal): ± 0.1%, Sensitivity: 0.02 µW, Chemistry Administration.
- SEM device: FEI Quanta FEG 250, accelerating voltage of 20 kV, spot size 3.5 nm and Circular Backscatter (CBS) Detector. Desert Research Center.

2.3. METHODS:

Three distinct types of Triketones (TKs) were synthesized through reactions of Dimedone with three specific acids: Adipic Acid, Azelaic Acid, and Glutaric Acid. Subsequently, these TKs underwent reactions with TREN, leading to the formation of

Poly(diketoenamine) (PDK) vitrimers. These PDK vitrimers were then employed to create three types of composites by interacting with Carbon Nanotubes (CNTs). The resulting PDKs and their composites were subsequently blended with PVC. Table 1 provides the mole fractions and wt % for each compound.

Table 1: Coding of prepared compounds and vitrimers.

	Cpds/mole	Dimedone	Adipic	Azelaic	Glutaric	DMAP	DCC	PDK Vitrimers	TREN	CNT	PVC
		(mol)	(mol)	(mol)	(mol)	(mol)	(mol)	(mol)	(mol)	(%)	(%)
Basic compounds	TK-AD	2.1	1			3	2.4				
	TK-AZ	2.1		1		3	2.4				
	TK-G	2.1			1	3	2.4				
PDK Vitrimers	PDK-TK-AD							1	1		
	PDK-TK-AZ							1	1		
	PDK-TK-G							1	1		
Vitrimer Composites	PDK-TKAD-CNT									3	
	PDK-TKAZ-CNT									3	
	PDK-TKG-CNT									3	
PDK Vitrimer blends	PDK-TK-AD-PVC										10
	PDK-TK-G-PVC										10
	PDK-TK-AD-CNT-PVC										10
	PDK-TK-G-CNT-PVC										10

Abbreviations in **table 1: AD** for Adipic acid, **AZ** for Azelaic acid, **G** for Glutaric acid, **DMAP** for 4-dimethylaminopyridine, **DCC** for N,N'-dicyclohexylcarbodiimide, **TREN** for tris(2-aminoethyl)amine, **PVC** for Polyvinyl Chloride.

General method for synthesis of Triketones:
Add Dimedone (2.1 mol) (1.0 M), Acid (1 mol), and 4-dimethylaminopyridine (DMAP) (3 mol) in 21 ml dichloromethane with stirring at room temperature. A separate solution of N, N'-dicyclohexylcarbodiimide (DCC) (2.4 mol) (1.0 M) in 24 ml dichloromethane was adding slowly at room temperature to the reaction mixture. The reaction progress for 4 h with stirring at room temperature. The dichloromethane filtrate was collected and washed with few of 3% Hydrochloric acid (HCl) until the pH of the aqueous phase was < 3. The organic phase was separated and dried over $MgSO_4$ then filtered. The solvent was removed under vacuum. The solid was recrystallized from mixture of ethyl acetate and hexane (ETOAc/Hex) to yield crystals [17].

2.3.1. Synthesis method of 2-[6-(4,4-dimethyl-2,6-dioxocyclohexyl)-6-oxohexanoyl]-5,5-dimethylcyclohexane-1,3-dione:

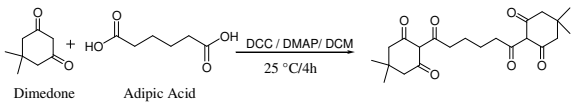

Dimedone Adipic Acid TK-AD

Equation 1: Synthesi of TK-AD

2.3.2. Synthesis method of 2-[9-(4,4-dimethyl-2,6-dioxocyclohexyl)-9-oxononanoyl]-5,5-dimethylcyclohexane-1,3-dione:

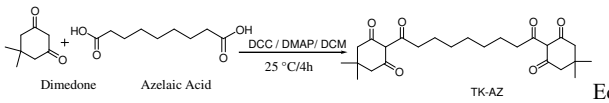

Dimedone Azelaic Acid TK-AZ

Equation 2: Synthesis of TK-AZ.

2.3.3. Synthesis method of 2-[5-(4,4-dimethyl-2,6-dioxocyclohexyl)-5-oxopentanoyl]-5,5-dimethylcyclohexane-1,3-dione:

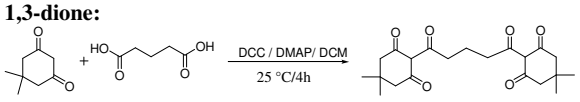

Dimedone Glutaric Acid TK-G

Equation 3: Synthesis of TK-G.

General method for synthesis of Diketoneamine Polymer (PDK):
PDK synthesis occurred by the Polycondensation reaction of ß-triketones with aliphatic amines to give Diketoenamine network polymers. The method in general for all reactions occurred by dissolving a specific amount of triketone dimer (TK) (1 mol) in a suitable organic solvent, then adding tris(2-aminoethyl)amine (TREN) (1 mol) with stirring for couple of hours.

2.3.4. Synthesis method of PDK-TK-AD:

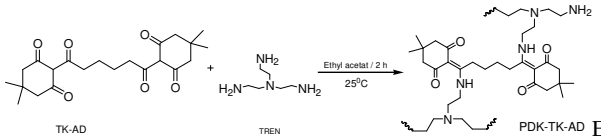

Equation 4: Synthesis of PDK-TK-AD.

2.3.5. Synthesis method of PDK-TK-AZ:

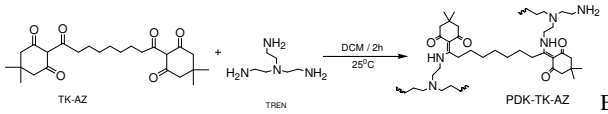

Equation 5: Synthesis of PDK-TK-AZ.

2.3.6. Synthesis method of PDK-TK-G:

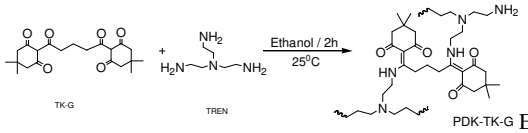

Equation 6: Synthesis of PDK-TK-G

General method for synthesis of Polydiketone Vitrimer nanocomposite:

The optimal weight proportion of carbon nanotubes (CNTs) in polyketone (POK) has been established as 3%, as reported by Seki [44]. Accordingly, polydiketone vittrimer nanocomposites incorporating 3% CNTs into the polydiketone matrix at room temperature have demonstrated considerable potential. Based on this optimal CNT content, we have synthesized the following nanocomposites: PDK-TK-AD-CNT, PDK-TK-AZ-CNT, and PDK-TK-G-CNT.

2.3.7. PVC Blend Preparation:

Based on the optimal 10% PDK content [45], the preparation of the PVC-polydiketone (PDK) nanocomposite blend involved dissolving 1 gram of PVC in cyclohexanone and 0.1 gram of PDK (or its composite) in ethanol. The two solutions were then thoroughly mixed, and the solvent was evaporated at 60 °C to yield the final blend.

3. Results and Discussion

Triketones compounds were prepared by condensation reaction of methylene group of Dimedone with hydroxyl group of acids respectively: Adipic Acid, Azelaic Acid, and Glutaric Acid producing TK-AD, TK-AZ, and TK-G releasing H_2O as by product at room temperature.

TK-AD Triketone compound was prepared and gave a yield of 86.84 %, and it was characterized and gave the following results: EI MASS for $C_{22}H_{30}O_6$ (M) calculated 390.47, the spectrum showed high intensity peak at 391.9 which referred to the molecular weight of TK-AD, FT-IR (neat): 2956.19, 2870.68 (CH, aliphatic), 1657.46 (CO) cm^{-1}. ^{1} H NMR (500 MHz, $CDCl_3$): 3.07 (s, 4H, CH_2), 2.54 (s, 4H, CH_2), 2.36 (s, 4H, CH_2), 1.72 (m, 4H, CH_2), 1.09 (s, 12H, CH_3) ppm, there is a peak appear at 18 for (s, 2H, CH) [17] but it out of scale.

TK-AZ Triketone compound was prepared and gave a yield of 83.65 %, and it was characterized and gave the following results: EI MASS for $C_{25}H_{36}O_6$ (M) calculated 432.55, the spectrum showed high intensity peak at 433.32 which referred to the molecular weight of TK-AZ**,** FT-IR (neat): 2868.04, 2855.95 (CH, aliphatic), 1665.16 (CO) cm^{-1}. ^{1} H NMR (500 MHz, $CDCl_3$): 2.94 (s, 4H, CH_2), 2.46 (s, 4H, CH_2), 2.30 (m, 4H, CH_2), 1.58 (m, 4H, CH_2), 1.54 (m, 4H, CH_2), 1.29 (m, 2H, CH_2), 1.01 (s, 12H, CH_3) ppm**,** there is a peak appear at 18 for (s, 2H, CH) [17] but it out of scale.

TK-G Triketone compound was prepared and gave a yield of 79.83 %, and it was characterized and gave the following results: EI MASS for $C_{21}H_{28}O_6$ (M) calculated 376.44, the spectrum showed high intensity peak at 377.16 which refered to the molecular weight of TK-G**,** FT-IR (neat): 2956.46, 2869.56 (CH, aliphatic), 1663.99 (CO) cm^{-1}**.** ^{1} H NMR (500 MHz, $CDCl_3$): 3.08 (s, 4H, CH_2), 3.05 (s, 4H, CH_2), 2.37 (m, 4H, CH_2), 1.93 (m, 2H, CH_2), 1.04 (s, 12H, CH_3) ppm, there is a peak appear at 18 for (s, 2H, CH) [17] but it out of scale.

The synthesis of PDK vitrimers was carried out through a polycondensation reaction between β-triketones and aliphatic amine (TREN) in an appropriate organic solvent, resulting in the formation of diketoenamine network polymers.

PDK-TK-AD vitrimer was prepared and gave yield of 94.74 %, and it was characterized and gave the following results: EI MASS spectrum showed high intensity peaks at 501.34, 751.50, and 1002.38 which referred to the molecular weights of fragments of PDK-TK-AD vitrimer. FT-IR (neat): 3446.99 (NH), 2929.89, 2858.07 (CH, aliphatic), 1630.76 (CO) cm^{-1}. ^{1} H NMR (500 MHz, $CDCl_3$): 13.21 (s, 1H, NH), 5.75 (s, 4H, CH_2), 4.61 (s, 4H, CH_2), 4.3(broad s, 1H, NH), 3.54 (m, 4H, CH_2),

2.93 (m, 4H, CH_2), 2.66 (m, 4H, CH_2), 2.16 (m, 4H, CH_2), 1.68 (m, 4H, CH_2), 1.27 (m, 4H, CH_2), 0.88 (s, 12H, CH_3) ppm, Density of PDK of Tk6 = 1.165 g/cm^3, Melting Point over 300 °C.

PDK-TK-AZ vitrimer was prepared and gave yield of 74.35 %, and it was characterized and gave the following results: EI MASS spectrum showed high intensity peaks at 794.55, 1086.77, and 1108.20 which referred to the molecular weights of fragments of PDK-TK-AZ vitrimer. FT-IR (neat): 3432.63 (NH), 2929.89, 2853.28 (CH, aliphatic), 1630.76 (CO) cm^{-1}. ^{1}H NMR (500 MHz, $CDCl_3$): 13.28(s, 1H, NH), 5.76 (s, 4H, CH_2), 5.65 (s, 4H, CH_2), 4.06 (broad s, 1H, NH), 3.31 (m, 4H, CH_2), 2.97 (m, 4H, CH_2), 2.64 (m, 4H, CH_2), 2.51 (m, 4H, CH_2), 2.21 (m, 4H, CH_2), 1.61 (m, 4H, CH_2), 1.37 (m, 4H, CH_2), 1.31 (m, 2H, CH_2), 1.23 (s, 12H, CH_3) ppm**,** Density of PDK-TK-AZ = 1.112 g/cm^3, Melting Point over 300 °C.

PDK-TK-G vitrimer was prepared and gave yield of 70.86 %, and it was characterized and gave the following results: EI MASS spectrum showed high intensity peaks at 655.46, and 1197.84 which refered to the molecular weights of fragments of PDK-TK-AG vitrimer. FT-IR (neat): 3427.84 (NH), 2934.68, 2843.71 (CH, aliphatic), 1635.55 (CO) cm^{-1}**.** ^{1}H NMR (500 MHz, $CDCl_3$): 13.18 (s, 1H, NH), 6.98 (s, 4H, CH_2), 6.6 (s, 4H, CH_2), 5.75 (m, 4H, CH_2), 3.85 (broad s,1H, NH), 2.95 (m, 4H, CH_2), 2.65 (m, 4H, CH_2), 2.18 (m, 4H, CH_2), (m, 4H, CH_2), 1.69 (m, 4H, CH_2), 1.28 (m, 2H, CH_2), 0.96 (s, 12H, CH_3) ppm**,** Density =1.162 g/cm^3, Melting Point over 300 °C.

The results from FTIR and ^{1}H NMR spectroscopy reveal distinct differences between triketones (TKs) and poly(diketoenamine) vitrimers (PDKs). Specifically, in the FTIR spectra, a new peak appears in the PDKs' spectrum near 3400 cm^{-1}, corresponding to the amine (NH_2) group. In the ^{1}H NMR spectra, two new peaks emerge in the PDKs' spectrum at approximately 13 and 4 ppm, attributed to the NH and NH_2 groups, respectively. These spectral changes indicate a polycondensation reaction between β-TKs and aliphatic amine (TREN), leading to the formation of PDK vitrimers.

Thermogravimetric analysis (TGA):

The thermal behavior of PDK vitrimers are studied using TGA and Differential Scanning Calorimetry (DSC) to assess their stability and decomposition under heat. Thermal stability is essential for applications; they are evaluated from room temperature to 600°C in nitrogen sphere.

PDK-TK-AD: the TGA curve demonstrates complete decomposition in a nitrogen atmosphere up to 600°C, with two key weight-loss stages. The first stage (room temperature to 206°C) reflects a 7.7% weight loss due to unreacted light hydrocarbons, confirmed by FT-IR analysis which revealed shared peaks at (1400 - 1500 cm^{-1}) between TK-AD and PDK-TK-AD. The second stage (206–506°C) indicates a 38.3% weight loss attributed to polymer decomposition. The DTA curve highlights four endothermic peaks at 150°C, 206°C, 326°C, and 506°C, each representing significant decomposition events, fig.5.

PDK-TK-AZ: the TGA curve shows complete decomposition in a nitrogen atmosphere up to 564°C, with two weight-loss stage (room temperature to 204°C) indicates a 5.32% weight loss due to unreacted light hydrocarbons, confirmed by FT-IR analysis which revealed shared peaks at (1400 - 1500 cm^{-1}) between TK-AZ and PDK-TK-AZ, indicating the presence of these hydrocarbons. The second stage (204–529°C) shows a 54% weight loss from polymer decomposition. The DTA curve supports this, with endothermic peaks at 204°C, 348°C, and 479°C, signifying decomposition events, fig.6.

PDK-TK-G: the TGA curve shows complete decomposition in a nitrogen atmosphere at 566°C, with two weight-loss stages. The first stage (room temperature to 191°C) results in a 7% weight loss due to unreacted light hydrocarbons, confirmed by FT-IR analysis which revealed shared peaks at (1400 - 1500 cm^{-1}) between TK-G and PDK-TK-G, indicating the presence of these hydrocarbons. The second stage (191–491°C) involves a 49% weight loss from polymer decomposition. The DTA curve highlights three endothermic peaks at 161°C, 323°C, and 430°C, marking significant decomposition events, fig.7.

PDK-TK-AD-CNT: the TGA curve shows complete decomposition in a nitrogen atmosphere at 563°C, with two weight-loss stages. The first stage (room temperature to 206°C) results in a 7.3% weight loss due to unreacted light hydrocarbons affecting polymer yield. The second stage (206–593°C) reflects a 43.9% weight loss linked to polymer decomposition. The DTA curve identifies four endothermic peaks at 143°C, 331°C, 413 °C, and 593°C, marking decomposition events, fig.8.

PDK-TK-AZ-CNT: the TGA curve shows complete decomposition in a nitrogen atmosphere at 566.5°C, with two weight-loss stages. The first stage (room temperature to 177°C) reflects a 4.34% weight loss due to unreacted light hydrocarbons during polymer formation. The second stage (177–501.7°C) shows a 49.34% weight loss from polymer decomposition. The DTA curve highlights endothermic peaks at 133°C, 177°C, 352°C, and 471°C, indicating decomposition events, fig.9.

PDK-TK-G-CNT: the TGA curve indicates complete decomposition in a nitrogen atmosphere at 592°C, with two distinct weight-loss stages. The first stage (room temperature to 204°C) shows a 9.9% weight loss due to unreacted light hydrocarbons from the polymer formation. The second stage (204–516°C) reveals a 43.84% weight loss linked to partial decomposition. The DTA curve highlights two endothermic peaks at 117°C and 347°C, marking decomposition events, fig.10.

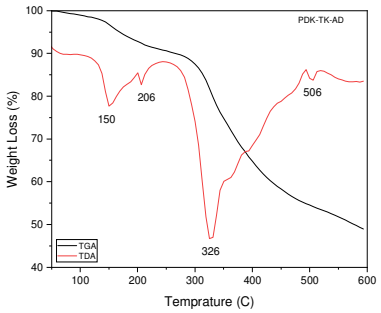

Figure 5: TGA thermogram of PDK-TK-AD

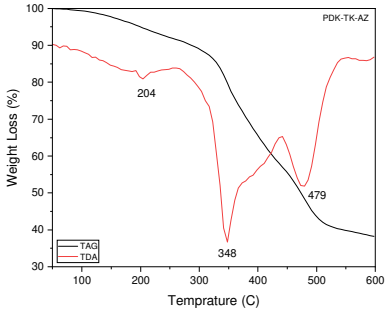

Figure 6: TGA thermogram of PDK-TK-AZ

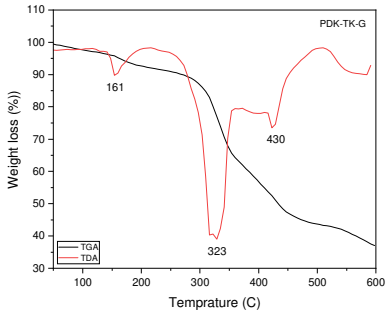

Figure 7: TGA thermogram of PDK-TK-G

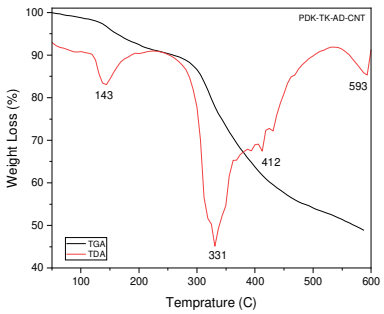

Figure 8: TGA thermogram of PDK-TK-AD-CNT

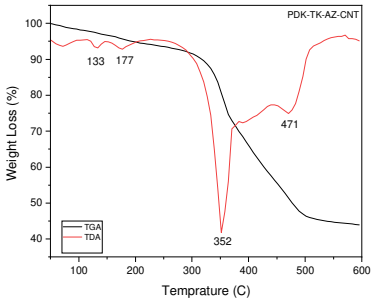

Figure 9: TGA thermogram of PDK-TK-AZ-CNT

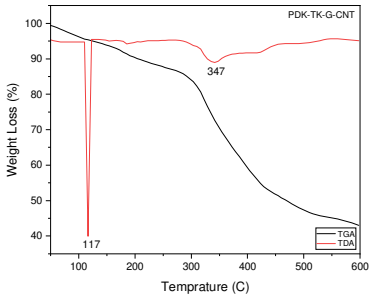

Figure 10: TGA thermogram of PDK-TK-G-CNT

It can be concluded that PDK-TK-AZ and its CNT composite exhibit exceptional thermal stability compared to the other samples investigated, as shown in Table 2. This makes them highly promising candidates for industrial applications that demand high-temperature durability. The enhanced performance is attributed to the unique chemical structure of PDK-TK-AZ, which strengthens intermolecular forces and promotes robust cross-linking within the polymer matrix, thereby significantly improving its thermal resilience.

Table 2: First and second degradation peaks for prepared materials from DTA thermograms.

Material	First Degradation Peak	Second Degradation Peak
PDK-TK-AD	326 °C	506 °C
PDK-TK-AZ	348 °C	479 °C
PDK-TK-G	323°C	430 °C
PDK-TK-AD-CNT	331 °C	593 °C
PDK-TK-AZ-CNT	352 °C	471 °C
PDK-TK-G-CNT	347 °C	508 °C

Differential Scanning Calorimetry (DSC):

It is directly measures heat flow differences between a sample and a reference, providing essential insights into phase transitions such as melting, glass transition, and chemical reactions like curing or decomposition. The glass transition temperature (T_g) was determined for PDK-TK-AD, PDK-TK-AZ, PDK-TK-G, and their CNT composites (PDK-TK-AD-CNT, PDK-TK-AZ-CNT, PDK-TK-G-CNT). Notably, no evidence of crystallization phase transitions was detected in any of the samples.

In figures 11, 12 glass transition temperatures (T_g) for PDK-TK-AD-CNT and PDK-TK-AZ-CNT are higher than that of PDK-TK-AD and PDK-TK-AZ due to presence of CNT which increase PDKs nanoscale, surface area, and intermolecular forces that need higher forces than the pristine PDKs.[46].

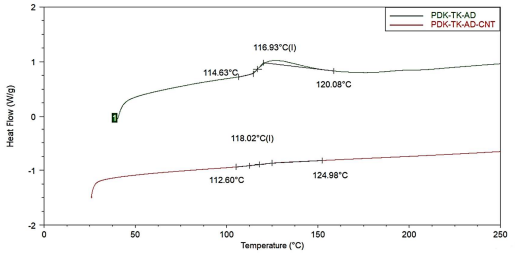

Figure 11: DSC thermogram of PDK-TK-AD and its nanocomposite

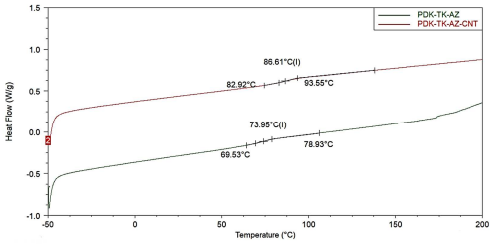

Figure 12: DSC thermogram of PDK-TK-AZ and its nanocomposite

But in case of PDK-TK-G and PDK-TK-CNT, T_g of CNT composite is lower than the pristine due to the crowding of chemical structure for PDK-TK-G that decrease PDK-TK-CNT nanoscale, surface area, and intermolecular forces. Plasticization Effect of CNTs which cause disrupting the regular packing of the polymer chains and increasing their mobility, and CNTs can alter the interfacial interactions between polymer chains, making the overall structure less rigid and more flexible, fig. 13.

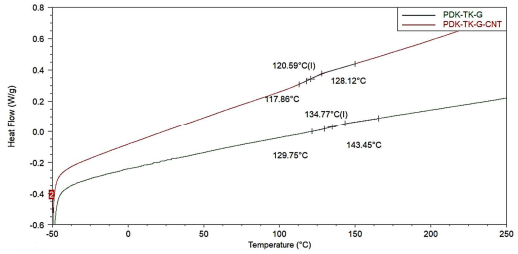

Figure 13: DSC thermogram of PDK-TK-G and its composite with CNT.

Polymer architecture plays a crucial role in determining the glass transition temperature (T_g). The polymers investigated in this study share a similar structure, differing primarily in the length of the hydrocarbon chain linking the two aromatic rings (1,3-cyclohexandione). Shorter hydrocarbon chains increase molecular crowding, intermolecular forces, interchain attraction, and cohesion, which in turn reduces the free volume and leads to a higher T_g. Based on this, the T_g order observed is PPDK-TK-G > PDK-TK-AD > PDK-TK-AZ.

The effect of carbon nanotubes (CNTs) on T_g depends on the polymer type, with measurements indicating both increases (suggesting reduced chain mobility) and decreases (indicating increased chain mobility) in T_g. For the CNT-reinforced polymers in this study, the T_g follows the same trend as the unreinforced polymers, but the values are higher due to the addition of CNTs. As such, the T_g order for the CNT composites is PPDK-TK-G-CNT > PDK-TK-AD-CNT > PDK-TK-AZ-CNT, as summarized in Table 3.

Table 3: Glass transition temperature (T_g) for prepared materials

Material	T_g	Figure No.
PDK-TK-AD	116.93 °C	FIG. 11
PDK-TK-AZ	73.95 °C	FIG. 12
PDK-TK-G	134.77 °C	FIG. 13
PDK-TK-AD-CNT	118.02 °C	FIG. 11
PDK-TK-AZ-CNT	86.61 °C	FIG. 12
PDK-TK-G-CNT	120.59 °C	FIG. 13

Scanning Electron Microscopy (SEM):

Scanning Electron Microscopy (SEM) analysis revealed distinct morphologies for the triketone compounds, polydiketone polymers, and their CNT composites. TK-AD forms rod-shaped clusters, while PDK-TK-AD displays large, flat flakes as a result of polycondensation with TREN, a finding confirmed by spectroscopic analysis. Upon incorporating CNTs into PDK-TK-AD, a homogeneous surface with embedded particles is observed. Similarly, TK-AZ forms sheet-like clusters, with PDK-TK-AZ presenting small flaky particles, while PDK-TK-AZ-CNTs exhibit a uniform surface featuring entangled threads due to the integration of CNTs. TK-G demonstrates uniform shapes, which transition into angular particles in PDK-TK-G after polycondensation. PDK-TK-G-CNTs show scattered spherical particles, with CNTs disrupting polymer chain packing and increasing free volume, confirming the formation of the composite. These observations highlight the structural transitions and the influence of CNT integration on morphology, as depicted in fig. 14.

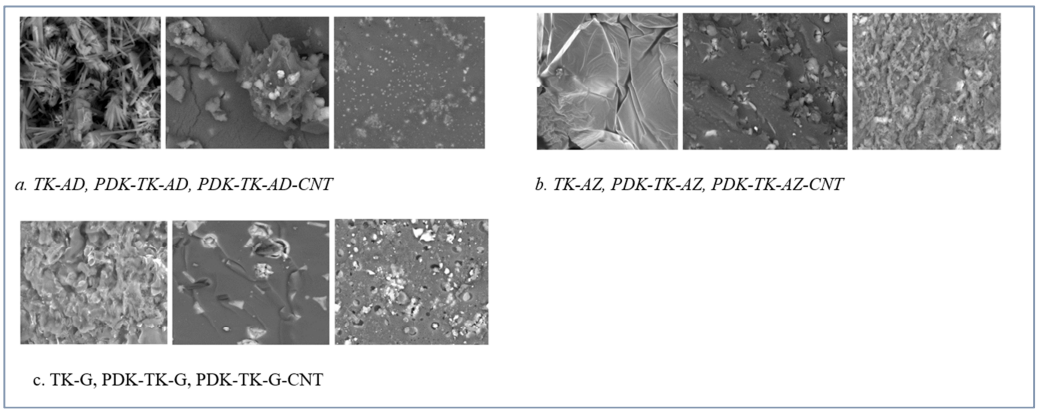

Figure 14: SEM of Triketones, Polydiketones, and its Nanocomposites

Application:

Polydiketone (PDK) vitrimers, characterized by dynamic covalent bonds, combine the durability of thermosets with the recyclability of thermoplastics. The incorporation of nanocarbon materials into vitrimer composites further enhances their mechanical strength, thermal stability, and electrical conductivity, rendering them highly suitable for high-performance applications. [47].

Blending PDK and its nanocarbon composites with polyvinyl chloride (PVC) enhances its thermal properties, particularly the glass transition temperature (T_g). PVC, a versatile thermoplastic, benefits from improved mechanical and thermal stability when incorporated with nanoscale fillers like CNTs or graphene [47]. Based on the optimal 10% PDK content [48], blends such as PDK-TK-AD–PVC, PDK-TK-AD-CNT–PVC, PDK-TK-G–PVC, and PDK-TK-G-CNT–PVC were prepared. These blends take advantage of the higher T_g of PDK, ensuring enhanced structural integrity at elevated temperatures.

Characterization:

In the IR analysis of PVC, characteristic peaks are observed at 606 cm^{-1} for the C-Cl bond, 1426 cm^{-1} for CH_2 wagging, and 2910 cm^{-1} for C-H stretching, which correspond to its typical vibrational modes. These distinctive peaks persist in the IR spectra of the PVC blends with Polydiketones and their Nanocomposites, indicating good compatibility between the components. This suggests that the blending process was successful, as shown in figures 15–17.

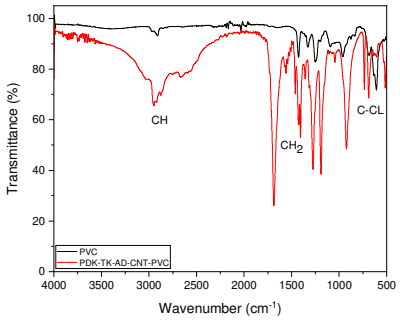

Figure 15: IR spectra of PVC and PDK-TK-AD-CNT-PVC

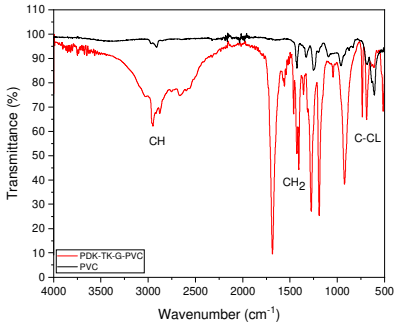

Figure 16: IR spectra of PDK-TK-G-PVC and PVC

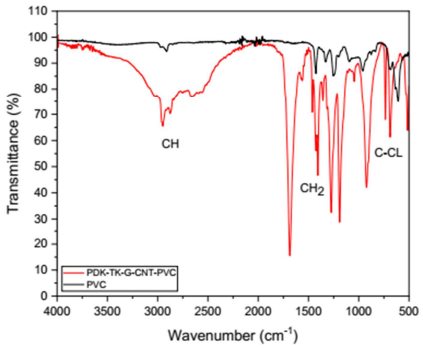

Figure 17: IR spectrum of PDK-TK-G-CNT-PVC and PVC

Differential Scanning Calorimetry (DSC) results offer valuable insights into the thermal stability and processing behavior of materials. Pure PVC exhibits a glass transition temperature (T_g) of approximately 86.37°C. Upon blending with polydiketones, the T_g increases, indicating enhanced compatibility and intermolecular interactions between PVC and the polydiketone or its nanocomposites, which restrict molecular mobility. The PDK-TK-G-PVC blend demonstrates the highest T_g at 141.45°C, attributed to strong intermolecular forces and reduced molecular mobility. However, the incorporation of PDK-TK-G-CNT into the PVC matrix results in a lower T_g of 128.91°C. This decrease is likely due to the crowding of PDK-TK-G's chemical structure, which reduces the nanoscale surface area and intermolecular forces, the plasticizing effect of CNTs disrupting the polymer's packing, and altered interfacial interactions that increase chain flexibility. These findings underscore the potential to tailor PVC's thermal properties by blending it with polydiketones and their nanocomposites, highlighting their relevance in the design of advanced materials for high-temperature applications. The T_g hierarchy is summarized in Table 4 and fig. 18.

Table 4: Glass transition temperature of PVC and its blends

Material	T_g	Figure No.
PVC	86.37 °C	18.a
PDK-TK-AD-PVC (PVC- 1)	131.14 °C	18.b
PDK-TK-G-PVC (PVC- 2)	141.45 °C	18.c
PDK-TK-AD-CNT-PVC (PVC- 3)	137.20 °C	18.d
PDK-TK-G-CNT-PVC (PVC- 4)	128.91 °C	18.e

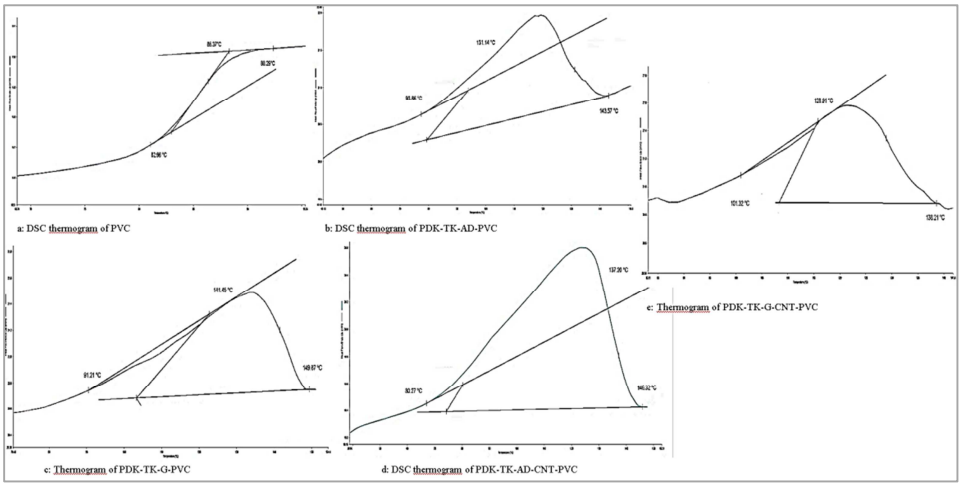

Figure 18: DSC thermograms of PVC's blends.

The inherent limitation of pure PVC is its relatively low glass transition temperature (T_g) of approximately 86.37°C, which compromises its thermal stability, leading to structural softening, deformation, and reduced mechanical strength at elevated temperatures. As a result, pure PVC is unsuitable for applications that require prolonged exposure to heat. To overcome these limitations, PVC blends with higher T_g values have been developed, significantly improving their thermal stability. These blends (PVC-1, PVC-2, PVC-3, and PVC-4) can be well-suited for integration into various high-performance applications, including:

1. **Building and Construction**: Enhanced thermal resistance for pipes, window frames, and roofing materials.
2. **Automotive Industry**: Improved heat resistance in interior components, under-the-hood parts, and electrical insulation.
3. **Packaging**: Greater compatibility with materials that require higher processing temperatures.
4. **Aerospace and Defense**: Reliable functionality in components and equipment exposed to extreme temperatures.

These advancements emphasize the critical role of blending PVC with polymers such as polydiketones to achieve superior thermal properties tailored for demanding applications.

4. Conclusion:

This study focused on the synthesis of novel triketone-based vitrimers, including polydiketone (PDK) vitrimers and carbon nanotube (CNT) composites, which were blended with polyvinyl chloride (PVC) to significantly enhance its thermal properties. Pure PVC, with a glass transition temperature (T_g) of 86.37°C, is susceptible to thermal softening, which limits its structural integrity and performance in high-temperature environments. However, blending PVC with PDK vitrimers led to a remarkable increase in the T_g, with PDK-TK-G-PVC (PVC-2) achieving a T_g of 141.45°C. This improvement is attributed to the enhanced intermolecular forces and exceptional compatibility between the PDK and PVC components, which reinforce the polymer matrix. In contrast, the PDK-TK-G-CNT-PVC (PVC-4) blend showed a slightly lower T_g of 128.91°C, likely due to the plasticizing effect of CNTs, which disrupt the molecular packing and reduce the overall rigidity of the composite. These results suggest that while CNTs improve certain aspects of the material, their presence can also influence the polymer's thermal properties in a manner that must be carefully optimized for specific applications [47, 48].

This innovative approach not only enhances PVC's thermal properties but also significantly broadens its potential for integration into a wide range of engineering applications, including those requiring materials with exceptional heat resistance. The findings emphasize the transformative role of PDK vitrimers and their composites in advancing the development of high-performance materials, with superior thermal stability. By improving the thermal properties of PVC, this research opens new possibilities for its use in demanding environments. This work supports industry by fostering material innovation, enabling the creation of next-generation composites that can withstand extreme conditions, and ultimately enhancing the performance, reliability, and longevity of products across diverse fields. Moreover, it paves the way for future research focused on tailoring the properties of polymer blends for specialized applications.

Conflicts of interest:

There is no conflict to declare.

References:

1. Montarnal, D.; Capelot, M.; Tournilhac, F.; Leibler, L. Silica-Like Malleable Materials from Permanent Organic Networks. Science, 2011, 334, 965–968.
2. Jin, Y.; Lei, Z.; Taynton, Ph.; Huang, S.; Zhang, W. Malleable and Recyclable Thermosets: The Next Generation of Plastics. Matter., 2019, 1, 1456–1493.
3. Alkonis, J. J.; MacKnight, W. J. Introduction to Polymer Viscoelasticity, 2nd ed.; Wiley, 1983.
4. Doi, M. Introduction to Polymer Physics; Oxford University Press, 1996.
5. Odian, G. G. Principles of Polymerization, 4th ed.; Wiley, 2003.
6. Yang, Y.; Boom, R.; Irion, B.; van Heerden, D. J.; Kuiper, P.; de Wit, H. Recycling of Composite Materials. *Chem. Eng. Process. Process Intens., 2012, 51, 53–68.
7. Oliveux, G.; Dandy, L. O.; Leeke, G. A. Current Status of Recycling of Fibre Reinforced Polymers: Review of Technologies, Reuse and Resulting Properties. Prog. Mater. Sci., 2015, 72, 61–99.
8. Kloxin, C. J.; Scott, T. F.; Adzima, B. J.; Bowman, C. N. Covalent Adaptable Networks (CANs): A Unique Paradigm in Cross-Linked Polymers. Macromolecules, 2010, 43, 2643–2653.
9. Kloxin, C. J.; Bowman, C. N. Covalent Adaptable Networks: Smart, Reconfigurable and Responsive Network Systems. Chem. Soc. Rev., 2013, 42, 7161–7173.
10. Denissen, W.; Winne, J. M.; Du Prez, F. E. Vitrimers: Permanent Organic Networks with Glass-Like Fluidity. Chem. Sci., 2016, 7, 30–38.
11. Y. Jin, Z. Lei, Ph. Taynton, S. Huang, and W. Zhang, Malleable and recyclable thermosets: The next generation of plastics, Matter,2019, 1, 1456–1493.
12. Z. P. Zhang, M. Z. Rong, M. Q. Zhang, Polymer engineering based on reversible covalent chemistry: A promising innovative pathway towards new materials and new functionalities, Prog. Polym. Sci., 2018, 80, 39.
13. M. K. McBride, B. T. Worrell, T. Brown, L. M. Cox, N. Sowan, C. Wang, M. Podgorski, A. M. Martinez, C. N. Bowman, Enabling Applications of Covalent Adaptable Networks, Annu. Rev. Chem. Biomol., 2019, 10, 175.
14. M. Podgórski, B. D. Fairbanks, B. E. Kirkpatrick, M. McBride, A. Martinez, A. Dobson, N. J. Bongiardina, C. N. Bowman, Toward Stimuli-Responsive Dynamic Thermosets through Continuous Development and Improvements in Covalent Adaptable Networks (CANs), Adv. Mater., 2020, 32, 1906876.

15. E. Drent, J. A. M. van Broekhoven, and M. J. Doyle, J. Organomet. Efficient palladium catalysts for the copolymerization of carbon monoxide with olefins to produce perfectly alternating polyketones, Chem., 1991, 417, 235–251.
16. A. Sen, Mechanistic aspects of metal-catalyzed alternating copolymerization of olefins with carbon monoxide, Acc. Chem. Res., 1993, 26, 303–310.
17. P. R. Christensen, A. M. Scheuermann, K. E. Loeffler, B. A. Helms, Closed-loop recycling of plastics enabled by dynamic covalent diketoenamine bonds, Nature Chemistry, 2019, 11, 442–448.
18. Ma, Y., Li, R., Luo, S., Shen, X., Tao, R., Jin, Y., Zhang, W., & Qiu, L. Highly conductive poly(imide–imine) hybrid vitrimer-graphene aerogel composites. Chinese Journal of Chemistry, 2023, 41(17), 2125–2131.
19. Yang, X., Yue, N., Guo, X., Lu, B., Feng, Y., Huang, M., & Liu, C. Research progress in vitrimer-based carbon-fiber-reinforced composites and their molding methods. China Plastics, 2024, 38(10), 103–113.
20. Wang, Y., Liu, Y., Zhang, Z., Qi, Z., Zhang, C., Li, M., Wang, L., Yan, Z., Shang, L., & Ao, Y. Reprocessable, self-adhesive, and recyclable carbon fiber-reinforced composites using a catalyst-free self-healing bio-based vitrimer matrix. ACS Sustainable Chemistry & Engineering, 2024, 12(1), 123–135.
21. Kausar, A., & Ahmad, I. State-of-the-art epoxy vitrimer nanocomposites with graphene, carbon nanotube, and silica—fundamentals and applications. Journal of Reinforced Plastics and Composites, 2024, 43(9), 735–756.
22. Cortés, A., Sánchez-Romate, X. F., Martínez-Díaz, D., Prolongo, S. G., & Jiménez-Suárez, A. Recyclable multifunctional nanocomposites based on carbon nanotube reinforced vitrimers with shape memory and Joule heating capabilities. Polymers, 2024, 16(3), 388.
23. Z.P. Zhang, M.Z. Rong, M.Q. Zhang, Polymer engineering based on reversible covalent chemistry: a promising innovative pathway towards new materials and new functionalities, Prog. Polym. Sci., 2018, 80, 39–93.
24. M. Ahmad, S. Naz, Graphene-based composite nanostructures: synthesis, properties, and applications, Handbook of Graphene, River Street, Hoboken, USA, 2019, 4, 203–232.
25. S. Rathinavel, K. Priyadharshini, D. Panda, A review on carbon nanotube: An overview of synthesis, properties, functionalization, characterization, and the application, Materials Science and Engineering: B, 2021, 268, 115095.
26. P. Yan, W. Zhao, L. Jiang, B. Wu, K. Hu, Y. Yuan, J. Lei, Reconfiguration and shape memory triggered by heat and light of carbon nanotube-polyurethane vitrimer composites, J. Appl. Polym. Sci., 2018, (5), 135.
27. J. Zhang, Z. Lei, S. Luo, Y. Jin, L. Qiu, W. Zhang, Malleable and recyclable conductive mwcnt-vitrimer composite for flexible electronics, ACS Appl. Nano Mater., 2020, 3 (5), 4845–4850.
28. N. Lorwanishpaisarn, N. Srikhao, K. Jetsrisuparb, J.T. Knijnenburg, S. Theerakulpisut, M. Okhawilai, P. Kasemsiri, Self-healing ability of epoxy vitrimer nanocomposites containing bio-based curing agents and carbon nanotubes for corrosion protection, J. Polym. Environ., 2022, 30 (2), 472–482.
29. H. Fang, W. Ye, K. Yang, K. Song, H. Wei, Y. Ding, Vitrimer chemistry enables epoxy nanocomposites with mechanical robustness and integrated conductive segregated structure for high performance electromagnetic interference shielding, Compos. Part B: Eng., 2021, 215, 108782.
30. N. Zheng, Y. Xu, Q. Zhao, T. Xie, Dynamic Covalent Polymer Networks: A Molecular Platform for Designing Functions beyond Chemical Recycling and Self-Healing, Chem. Rev., 2021, 121, 1716–1745.
31. Y. Zhang, E. Yukiko, I. Tadahisa, Bio-Based Vitrimers from Divanillic Acid and Epoxidized Soybean Oil, RSC Sustain., 2023, 1, 543–553.
32. B. Xue, R. Tang, D. Xue, Y. Guan, Y. Sun, W. Zhao, J. Tan, X. Li, Sustainable Alternative for Bisphenol A Epoxy Resin High-Performance and Recyclable Lignin-Based Epoxy Vitrimers, Industrial Crops and Products, 2021, 168, 113583.
33. Y. Zhu, F. Gao, J. Zhong, L. Shen, Y. Lin, Renewable castor oil and DL-limonene derived fully bio-based vinylogous urethane vitrimers, European Polymer Journal, 2020, 135, 109865.
34. Z. Niu, R. Wu, Y. Yang, L. Huang, W. Fan, Q. Dai, L. Cui, J. He, C. Bai, Recyclable, robust and shape memory vitrified polyisoprene composite prepared through a green methodology, Polymer, 2021, 228, 123864.
35. Y. Tian, X. Feng, C. Wang, S. Shang, H. Liu, X. Huang, J. Jiang, Z. Song, H. Zhang, Fully Biobased Degradable Vitrimer Foams: Mechanical Robust, Catalyst-Free Self-Healing, and Shape Memory Properties, ACS Appl. Mater. Interfaces, 2024, 16 (5), 6523–6532.
36. Y. Yang, H. Wang, S. Zhang, Y. Wei, X. He, J. Wang, Y. Zhang, Y. Ji, Vitrimer-Based Soft Actuators with Multiple Responsiveness and Self-Healing Ability Triggered by Multiple Stimuli, Matter, 2021, 4 (10), 3354–3365.
37. N. Zheng, Y. Xu, Q. Zhao, T. Xie, Dynamic Covalent Polymer Networks: A Molecular Platform for Designing Functions Beyond Chemical Recycling and Self-Healing, Chem. Rev., 2021, 121 (3), 1716–1745.
38. H. Zhang, J. Cui, G. Hu, B. Zhang, Recycling Strategies for Vitrimers, Int. J. Smart Nano Mat., 2022, 1–24.
39. B. Krishnakumar, R.P. Sanka, W.H. Binder, V. Parthasarthy, S. Rana, N. Karak, Vitrimers: Associative Dynamic Covalent Adaptive Networks in Thermoset Polymers, Chem. Eng. J., 2020, 385, 123820.
40. H. Memon, Y. Wei, L. Zhang, Q. Jiang, W. Liu, An Imine-Containing Epoxy Vitrimer With Versatile Recyclability and Its Application in Fully Recyclable Carbon Fiber Reinforced Composites, Compos. Sci. Technol., 2020, 199, 108314.
41. J. Joe, J. Shin, Y.S. Choi, J.H. Hwang, S.H. Kim, J. Han, B. Park, W. Lee, S. Park, Y.S. Kim, D.G. Kim, A 4D printable shape memory vitrimer with repairability and recyclability through network architecture tailoring from commercial poly(epsilon-caprolactone), Adv. Sci., 2021, 8 (24), e2103682.
42. Z. Guo, W. Wang, K. Majeed, B. Zhang, F. Zhou, Q. Zhang, Fabrication of multi-functional bio-based vitrimer and conductive composites via ugi four-component polymerization, Colloids Surf. A: Physicochem. Eng. Asp., 2022, 129911.

43. Z. Guo, W. Wang, Z. Liu, Y. Xue, H. Zheng, K. Majeed, B. Zhang, F. Zhou, Q. Zhang, Preparation of carbon nanotube-vitrimer composites based on double dynamic covalent bonds: electrical conductivity, reprocessability, degradability and photo-welding, Polymer, 2021, 235, 124280.
44. Y. Seki, M. M. Tokgöz, F. Öner, M. Sarikanat, L. Altay, Carbon Nanotube-, Boron Nitride-, and Graphite-Filled Polyketone Composites for Thermal Energy Management, ACS Omega, 8, 19265−19272, 2023.
45. J. G. Bonner, Edinburgh, Scotland, Polymer blends of PVC and Polyketones, US Patent US5610236A, 1977.
46. M. Rahmat, P. Hubert, composite science and technology, 72 (1), 72-84, 2011.
47. Y. Hong, M. Goh, Vitrimer Nanocomposites for Highly Thermal Conducting Materials with Sustainability, *Polymers* 2024, *16*(3), 365.
48. H. Akhina, T. Sabu, Nanocomposite of PVC with CNT, 241-260, 2024.